NASA
Technical Memorandum 79123

AVRADCOM
Technical Report 79-12

EFFECTS OF STEADY-STATE PRESSURE DISTORTION ON THE STALL MARGIN OF A J85-21 TURBOJET ENGINE

George A. Bobula
Propulsion Laboratory
AVRADCOM Research and Technology Laboratories

and

Leo A. Burkardt
Lewis Research Center
Cleveland, Ohio

March 1979

1 Report No NASA TM 79123 AVRADCOM TR 79-12	2 Government Accession No	3 Recipient's Catalog No
4 Title and Subtitle **EFFECTS OF STEADY-STATE PRESSURE DISTORTION ON THE STALL MARGIN OF A J85-21 TURBOJET ENGINE**		5 Report Date March 1979 6 Performing Organization Code
7 Author(s) George A. Bobula and Leo A. Burkardt		8 Performing Organization Report No E-9958 10 Work Unit No
9 Performing Organization Name and Address NASA Lewis Research Center and AVRADCOM Research and Technology Laboratories Cleveland, Ohio 44135		11 Contract or Grant No 13 Type of Report and Period Covered Technical Memorandum
12 Sponsoring Agency Name and Address National Aeronautics and Space Administration Washington, D C. 20546 and U S. Army Aviation Research and Development Command, St Louis, Mo 63166		14 Sponsoring Agency Code
15 Supplementary Notes		

16 Abstract

An experimental investigation to determine the effects of the inlet pressure distortions, induced by five screen patterns, on the performance of a J85-21 turbojet engine was conducted at the NASA Lewis Research Center, Testing was in support of the HiMAT RPRV program at Dryden Flight Research Center Thus, distortion patterns were chosen based on anticipated application of test results to the HiMAT installation Tests were conducted at a simulated Mach number and altitude condition of 0.9 and 10 973 meters Results are presented in terms of distortion levels and standard compressor performance parameters.

17 Key Words (Suggested by Author(s))	18 Distribution Statement
Turbojet; Pressure distortion; Stall margin; Loss of stall margin; J85-21; HiMAT	Unclassified - unlimited STAR Category 07

19 Security Classif (of this report)	20 Security Classif (of this page)	21 No of Pages	22 Price*
Unclassified	Unclassified		

* For sale by the National Technical Information Service Springfield Virginia 22161

SUMMARY

An experimental investigation into the compressor stall margin loss of a J85-21 turbojet engine, due to screen-induced inlet pressure distortion, was performed at the NASA Lewis Research Center in support of the Highly Maneuverable Aircraft Technology Program. In these tests, five distortion patterns were compared with a clean-inlet configuration one was a graded tip-radial pattern; and the other four were one-per-rev type circumferential patterns, two complex and two graded. All tests were performed at simulated flight Mach number and altitude conditions of 0.9 and 10 973 meters.

The four one-per-rev type patterns lowered compressor performance along the operating line. The graded tip-radial distortion had no effect on the compressor stall line. Of the two complex one-per-rev patterns, which were geometrically similar but of different screen densities, the screen imposing the higher face average distortion level provided a larger stall margin loss. The two graded one-per-rev patterns, one having a higher maximum density and the other covering a greater overall extent, resulted in the same level of stall margin loss.

E-9958

INTRODUCTION

An experimental investigation was performed at the NASA Lewis Research Center to determine the compressor stall margin loss of a J85-21 turbojet engine due to inlet pressure distortions. The investigation was in support of the HiMAT RPRV program (refs. 1 to 4), being conducted by the NASA Hugh L. Dryden Flight Research Center.

The HiMAT RPRV uses a single J85-21 engine. The vehicle's air inlet is relatively short with substantial turning, and there has been concern over possible flow nonuniformity at the engine inlet, and its effect on engine operation. Available literature contained no information on the distortion tolerance of this engine, and unpublished data were not available. Thus, five inlet distortion screen patterns were chosen to gather experience and provide information to consider relative to the HiMAT installation. Two screens were complex one-per-rev patterns, two were graded one-per-rev patterns, and one was a graded tip-radial pattern. Base-line data were obtained with a clean inlet.

The testing was performed at a simulated flight Mach number and altitude condition of 0.9 and 10 973 meters (36 000 ft). Data were recorded along lines of constant corrected speed, ranging 90 and 104.5 percent Compressor stall was approached by decreasing the variable exhaust nozzle area while holding corrected speed fixed.

Results for each pattern are presented in terms of engine inlet flow quality and the resulting compressor performance. Inlet flow quality is indicated by various distortion-level parameters. Compressor performance is presented using the conventional parameters of pressure ratio, corrected airflow, and corrected speed.

APPARATUS AND PROCEDURE

Engine

The J85-21 engine is a 22 200-newton (5000-lb) thrust turbojet with afterburning, rated at 15 600-newton (3500-lb) thrust without afterburning. The engine has a nine stage axial compressor with variable inlet guide vanes and variable compressor stators in the first three stages. Its combustor is annular and discharges into a two-stage axial turbine. Exhaust products exit through a variable exhaust nozzle (VEN). (Symbols are defined in appendix A.)

The engine used in this program, S/N 225326, seen in figure 1, was a basically nominal J85-21, with the following exceptions: the afterburner fuel control was removed, the VEN was controlled through an analog computer which could provide either a standard nozzle schedule or independent nozzle control; the main fuel control was uptrimmed to allow engine operation at higher speeds than normal; the minimum VEN area was decreased for part of the test by adding six "mice," totaling 116 square centimeters (18 in^2), at the nozzle exit (fig. 2); and the standard turbine nozzle, having a flow area of 290.96 to 293.54 cm^2, was replaced with a reduced area stalling turbine nozzle, of flow area 212.56 cm^2, for a portion of the test. A further description of the engine may be found in references 5 and 6.

Installation

The engine installation is shown in figures 1 and 3. The installation was of a conventional direct-connect type, with the inlet bellmouth located in a plenum upstream of the engine chamber. A front bulkhead isolated the test chamber from the inlet plenum. Conditioned air was supplied to the inlet plenum to yield the desired engine inlet conditions. Engine exhaust products and test cell cooling air passed into an exhaust collector, which extended through a rear bulkhead. The test chamber altitude pressure was controlled by values downstream of the exhaust collector

Instrumentation

The instrumentation configuration for the data reported in this text is shown in figure 3. Engine airflow instrumentation consisted of temperatures measured at station 2.0 and pressures surveyed at station 1.0. Engine inlet and compressor exit conditions were measured in surveys at stations 2.0 and 3.0, respectively. Test chamber altitude pressure was based on the station 10 measurement of external static pressure at the nozzle exit.

Distortion Hardware

Engine inlet flow distortions were produced by placing various screen patterns across the inlet duct, one-duct diameter ahead of the engine inlet (fig. 3(a)). All screens were mounted on a support grid and backup

screen assembly. The support grid (fig. 4), was made of bars 0.151 cm (0.0595 in.) thick by 4.37 cm (1.72 in.) deep, spaced on 5.08 cm (2 in.) centerlines. The backup screen, (fig. 5(a)), consisted of 0.318 cm (0.125 in.) wire on 2.858 cm (1.125 in.) centerlines. The backup screen was rotated 57° clockwise from the support grid, when looking upstream.

The support grid and backup screen assembly comprised the baseline, or clean inlet, configuration with which five distortion patterns were compared. The five patterns tested are shown in figures 5 and 6. Screens numbered one and two were similar, complex circumferential patterns with number one providing greater blockage. Screens three and four were graded one-per-rev patterns. Pattern three was of 180° extent. Pattern four was of 120° extent but had greater blockage in its central region and a more severe step from clean to distorted regions than pattern 3. Screen five was a graded tip-radial pattern.

Test Procedures

During these tests, the average engine-inlet total pressure and total temperature, P_{t2} and T_{t2}, and the test chamber altitude pressure, P_{10}, were maintained at values corresponding to a simulated Mach number of 0.9 at an altitude of 10 973 meters (36 000 ft). Tests on each inlet configuration consisted of recording performance data along lines of constant corrected engine speed. Performance points were established by manually decreasing VEN in a stepwise manner, thus increasing compressor pressure ratio. A constant engine speed was maintained by varying the throttle position.

Steady-state performance points were recorded along constant speed lines until VEN closure resulted in a compressor stall. Occassionally, either a turbine temperature limit would be reached or VEN would be fully closed with no stall occurring. If turbine temperature was the limiting factor, this speed line was completed later with the reduced area turbine in place. When full nozzle closure did not stall the compressor, these stalls were attempted later with the VEN area reduced by adding the "mice" to the exhaust nozzle. Some tests required using both the "stalling turbine" and the VEN "mice" to stall the compressor.

With these methods, stall was achieved for all test configurations except with screen 4 at 102.5 and 104.5 percent corrected speeds. Operating line points on nominal VEN schedule, were recorded for the baseline clean inlet and all screen patterns except the graded tip-radial pattern 5.

Data Processing

All steady state performance data were recorded on the Lewis Central Automatic Digital Data Encoder (CADDE) (ref. 7). Compressor pressure ratio and corrected airflow were correlated with VEN position using this data. Compressor stall was located on a transient digital data record, and VEN position at stall was obtained. This value was then used with the above correlations to determine the compressor operating conditions at stall.

RESULTS AND DISCUSSION

Test results are presented in four inlet distortion pattern groupings. (1) clean inlet or baseline; (2) complex circumferential one-per-rev patterns; (3) graded circumferential one-per-rev patterns; and (4) graded tip radial pattern.

Inlet flow quality is discussed in terms of three parameters having the form $((P_{max} - P_{min})/P_{ave})$. These parameters, discussed in appendix B, are: (1) maximum circumferential distortion level $(\Delta P/P)_{cir,max}$; (2) face average circumferential distortion level $\overline{(\Delta P/P)_{cir}}$; and (3) radial distortion level $(\Delta P/P)_{rad}$. Distortion levels are presented as functions of corrected engine-inlet airflow.

Compressor performance resulting with the various distortion patterns is discussed and presented in terms of the conventional compressor parameters of pressure ratio, corrected inlet airflow, and corrected engine speed. Compressor stalling characteristics are presented in terms of clean inlet stall margin and loss of stall margin due to distortion. In this text, stall margin and loss in stall margin are defined as:

$$SM = \left[\frac{(P_{t,3}/P_{t,2})_{stall} - (P_{t,3}/P_{t,2})_{op.line}}{(P_{t,3}/P_{t,2})_{op.line}}\right]_{N/\sqrt{\theta}_2} \times 100.$$

and

$$LSM = \left\{1 - \frac{\left[(P_{t,3}/P_{t,2})_{stall} - (P_{t,3}/P_{t,2})_{op.line}\right]_{distorted}}{\left[(P_{t,3}/P_{t,2})_{stall} - (P_{t,3}/P_{t,2})_{op.line}\right]_{clean}}\right\}_{N/\sqrt{\theta}_2} \times 100.$$

where the subscript, $N/\sqrt{\theta}_2$, implies data are at a constant corrected engine speed.

For ease of presentation, only results for 100 percent corrected engine speed, 16 600 rpm, are discussed, these data are summarized in table I A summary of clean inlet stall margin is presented in table II.

Clean Inlet

Clean inlet, or baseline, distortion level and compressor performance are presented in figures 7 and 8, respectively. The corrected airflow at 100 percent $N/\sqrt{\theta}_2$ was 23.13 kg/sec, from table I, and distortion levels were $(\Delta P/P)_{cir,max} = 0.010$; $(\Delta P/P)_{cir} = 0.008$; and $(\Delta P/P)_{rad} = 0.011$. The resultant compressor operating point was at a pressure ratio of 7.74. Clean inlet stall occurred at a corrected airflow of 22.39 kg/sec and a pressure ratio of 8.89. Thus, the stall margin was 14.9 percent (table II).

Between 102.5 and 104.5 percent $N/\sqrt{\theta_2}$ the VEN schedule changed from PLA control to turbine temperature limiting. This is seen in the operating line changing slope abruptly above 102.5 percent $N/\sqrt{\theta_2}$ (fig. 8). This also occurred in most of the other operating lines investigated.

Complex, One-Per-Rev Circumferential Patterns

Inlet distortion levels resulting from the complex circumferential screen patterns 1 and 2, and the resulting compressor performance, are presented in figures 9 to 11. From table I, the $WA\sqrt{\theta_2}/\delta_2$ levels on the operating line at 100 percent $N/\sqrt{\theta_2}$ were 23.05 kg/sec with pattern 1 and 22.93 kg/sec with pattern 2. The maximum circumferential distortion level was 0.090 for both patterns. This parameter is the larger of the tip or hub region average distortion level, and ignores the central region of the inlet pressure profile. The face-average circumferential distortion level, however, weights all regions of the inlet pressure profile equally. For pattern 1 $(\Delta P/P)_{cir}$ was 0.077, while for pattern 2 it was 0.068. The radial distortion levels were very close for patterns 1 and 2, 0.022 and 0.021, respectively.

A comparison of the operating lines of the complex circumferential patterns with that of the clean inlet (fig. 10) shows mainly a movement of constant speed points to a lower pressure ratio and airflow with distortion. At 100 percent $N/\sqrt{\theta_2}$, the compressor with pattern 1 operated at a $P_{t,3}/P_{t,2}$ of 7.71 and with pattern 2 at 7.69. The compressor stall line was lowered more by the distortion from pattern 1 than it was by that from pattern 2. Stall occurred at a pressure ratio of 8.27 and a corrected airflow of 22.83 kg/sec with pattern 1, and at 8.37 and 22.60 kg/sec with pattern 2. Thus, as shown in figure 11, the loss in stall margin at 100 percent $N/\sqrt{\theta_2}$ was 51.6 percent with pattern 1 and 41.2 percent with pattern 2, and so, the severity of these complex, one-per-rev circumferential patterns with respect to stall margin loss, is more clearly indicated by $(\Delta P/P)_{cir}$.

Graded One-Per-Rev Patterns

Results of the tests with graded one-per-rev patterns 3 and 4 are shown in figures 12 to 14. With these patterns $(\Delta P/P)_{cir,max}$ was greater for the denser, 120°-extent screen 4, than for the 180°-extent screen 3. At 100 percent $N/\sqrt{\theta_2}$ on the operating line, with $WA\sqrt{\theta_2}/\delta_2$ of 22.77 kg/sec for pattern 3 and 22.91 kg/sec for pattern 4, the $(\Delta P/P)_{cir,max}$ levels were 0.093 and 0.107, respectively, see table I. The pressure defect due to pattern 4 was greatly dissipated in the central radii, however, and as a result $(\Delta P/P)_{cir}$ was greater for pattern 3 than for pattern 4, 0.090 versus 0.083. Radial distortion levels were very low for both patterns, 0.004 and 0.010, respectively. The operating lines of figure 13 again show a speed line shift, from the clean inlet case, to lower pressure ratio and corrected airflow. At 100 percent $N/\sqrt{\theta_2}$, the compressor operated at P_{t3}/P_{t2} and $WA\sqrt{\theta_2}/\delta_2$ of 7.67 and 22.77 kg/sec with pattern 3 and 7.66 and 22.91 kg/sec with pattern 4 The stall lines for patterns 3 and 4 were almost identical. It appears that the center dissipation of the smaller extent distortion compensated for its larger $(\Delta P/P)_{cir,max}$. The stalling

pressure ratio at 100 percent $N/\sqrt{\theta_2}$ was 8.11 for each patterns. $WA\sqrt{\theta_2}\delta_2$ was 22.51 kg/sec with pattern 3 and 22.56 kg/sec for pattern 4. The trade-off between circumferential extent and maximum distortion level resulted in nearly equal stall margin losses of 62.3 and 60.9 percent, respectively, as seen in figure 14

Graded Tip-Radial Pattern 5

Results of the tests with pattern 5, the graded tip-radial pattern, are shown in figures 15 to 17. Both measures of circumferential distortion were only slightly greater than clean inlet levels. The radial distortion level was 0.032 for $WA_1\sqrt{\theta_2}/\delta_2$ at 23.09 kg/sec, nearly three times clean inlet level.

Operating line data were not recorded with this screen pattern; however, since the lines of constant corrected speed and the stall line on figure 16 were nearly identical to the clean inlet map, the clean inlet operating line was assumed to approximate that for patter 5, for the purpose of calculating stall margin loss. Thus, in figure 17, the stall margin loss at 100 percent $N/\sqrt{\theta_2}$ is essentially zero.

SUMMARY OF RESULTS

An experimental investigation was conducted to determine the stall margin loss of a J85-21 turbojet engine compressor due to screen induced inlet pressure distortions. Tests were performed at a simulated flight Mach number and altitude condition of 0.9 and 10 973 meters. The principal results of this investigation follow, with observed pressure ratios and corrected airflows listed for engine operation at 100 percent corrected speed.

1. Compressor operating lines shifted to lower pressure ratio and corrected airflow conditions, but stayed on the normal operating line, when circumferential one-per-rev distortions were imposed on the baseline inlet configuration.

2. The complex circumferential pattern with the higher face average distortion level produced a larger stall margin loss than its geometrically similar, but less dense, counterpart.

3. The two graded one-per-rev patterns of different extents and screen densities produced the same stall margin losses. There was, therefore, a tradeoff between circumferential extent and maximum distortion level.

4. The graded tip-radial pattern had no effect on compressor performance.

APPENDIX A

SYMBOLS

HiMAT	Highly Maneuverable Aircraft Technology
LSM	loss in stall margin, percent
N	engine speed, rpm
P	pressure, N/cm^2
RPRV	remotely piloted research vehicle
SM	stall margin, percent
T	temperature, K
VEN	variable area exhaust nozzle
WA	engine airflow, kg/sec
$\triangle P/P$	distortion level
δ	ratio of total pressure to absolute pressure of NASA standard sea-level conditions
θ	ratio of total temperature to absolute temperature of NASA standard sea-level conditions

Superscript:

$\overline{\quad}$	face averaged value

Subscripts:

ave	average
cir	circumferential
clean	with a clean inlet
distorted	with a distorted inlet
max	maximum
min	minimum
N	at a constant speed
op.line	on the normal operating line
rad	radial
s	static condition
stall	on the stall line
t	total condition
1	airflow measurement location
2	engine inlet
3	compressor exit
10	nozzle exit, external or test chamber ambient

APPENDIX B

MEASUREMENT OF DISTORTION LEVEL

The engine inlet flow quality was based on a survey of 40 probes in an eight rake by five element per rake array. Rakes were located a 0°, 45°, 90°, 135°, 180°, 225°, 270°, and 315°. Each rake had its five probes located at centers of equal area between the inner wall at 6.91 cm (2.72 in.) and the outer wall at 23.0 cm (9.05 in.).

Circumferential pressure distortion parameters were developed by first calculating the average pressure minus minimum pressure for each ring, and dividing by the face average. Thus for ring a,

$$(\Delta P/P)_{cir,ring\ a} = \frac{(P_{t2,ring\ a})_{ave} - (P_{t2,ring\ a})_{min}}{P_{t2}}$$

$(\Delta P/P)_{cir,max}$ is then defined as the maximum of either the inner two or outer two ring distortion levels averaged. That is, with rings numbered 1 through 5 from outer to inner,

$$(\Delta P/P)_{cir,max} = Max\left[\frac{(\Delta P/P)_{cir,ring\ n} + (\Delta P/P)_{cir,ring\ n+1}}{2}\right]$$

where n = 1 or 4.

$\overline{(\Delta P/P)}_{cir}$ is simply the average of all five $(\Delta P/P)_{cir,ring\ a}$ values, or

$$\overline{(\Delta P/P)}_{cir} = \frac{1}{5}\sum_{n=1}^{5}(\Delta P/P)_{cir,ring\ n}$$

Radial distortion level is developed from a measurement of the tip and hub ring average pressures and the overall face average pressure It is defined as

$$(\Delta P/P)_{rad} = Max\left[\frac{P_{t2} - (P_{t2,ring\ n})_{ave}}{P_{t2}}\right]$$

where n = 1 or 5.

REFERENCES

1. Bellman, Donald R., and Kier, David A.· HiMAT - A New Approach to the Design of Highly Maneuverable Aircraft. SAE Paper 740859, Oct. 1974.

2. Bayati, Jamal E.: The HiMAT RPRV Propulsion Control System. SAE Paper 760887, Nov. 1976.

3. Lockenour, Jerry L., and Layton, Garrison P.: RPRV Research Focus on HiMAT. Astronautics and Aeronautics, vol. 14, Apr. 1976, pp. 36-41.

4. Taylor, John W. R., ed.: Jane's All the World's Aircraft. 1977-78, ed., Frankin Watts, Inc., 1977, pp. 670-671.

5. Taylor, John W. R., ed.· Jane's All the World's Aircraft. 1977-78 edition, Franklin Watts, Inc., 1977, p. 810.

6. J85-21 Training Guide. General Electric Co., Aircraft Engine Group, SEI-343, May 1972.

7. Central Automatic Data Processing System. NACA TN 4212, 1958.

8. Graber, Edwin J.; and Braithwaite, Willis M.: Summary of Recent Investigations of Inlet Flow Distortion Effect on Engine Stability. NASA TM X-71505, 1974.

TABLE I. - ENGINE OPERATION PARAMETERS AT 100 PERCENT $N/\sqrt{\theta_2}$

Operating line						Stall line	
Screen	P_{t3}/P_{t2}	$WA_1\sqrt{\theta_2}/\delta_2$ (kg/sec)	$(\Delta P/P)_{cir,max}$	$\overline{(\Delta P/P)}_{cir}$	$(\Delta P/P)_{rad}$	P_{t3}/P_{t2}	$WA_1\sqrt{\theta_2}/\delta_2$ (kg/sec)
Baseline	7.74	23.13	0.010	0.008	0.011	8.89	22.39
1	7.71	23.05	.090	.077	.022	8.27	22.83
2	7.69	22.93	.090	.068	.021	8.37	22.60
3	7.67	22.77	.093	.090	.004	8.11	22.51
4	7.66	22.91	.107	.083	.010	8.11	22.56
5	----------Not available----------					8.9	22.35

TABLE II. - CLEAN INLET STALL MARGIN

[Stall margin is defined for this text as the difference between the stall line pressure ratio and the operating line pressure ratio, both at the same corrected speed, divided by the operating line pressure ratio.]

$N/\sqrt{\theta_2}$	90, percent	95, percent	97.5, percent	100, percent	102.5, percent	104.5, percent
Stall margin, %	16.4	12.7	12.8	14.9	15.6	8.5

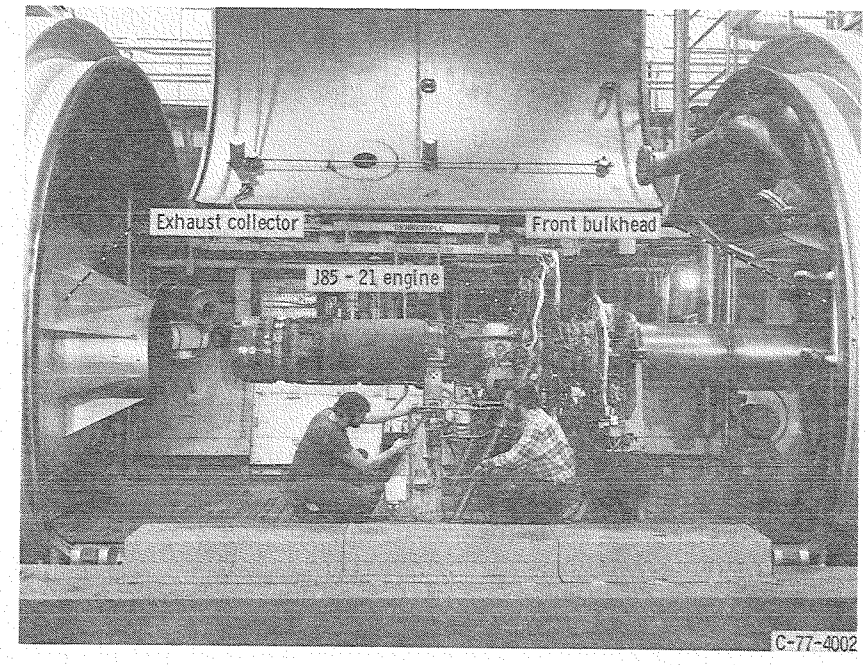

Figure 1. - J85-21 engine installation in altitude test chamber

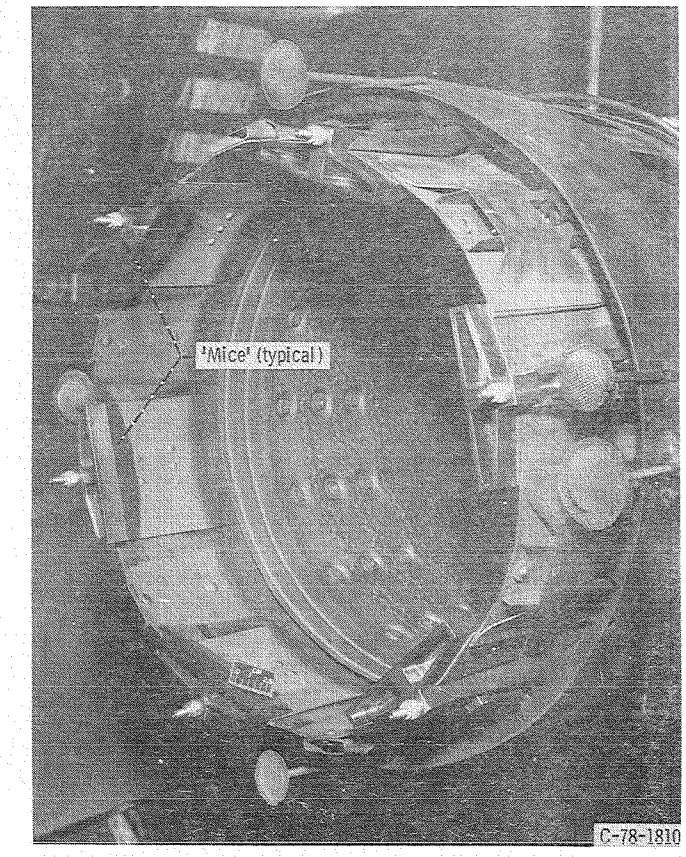

Figure 2. - 'Mice' installed on variable exhaust nozzle.

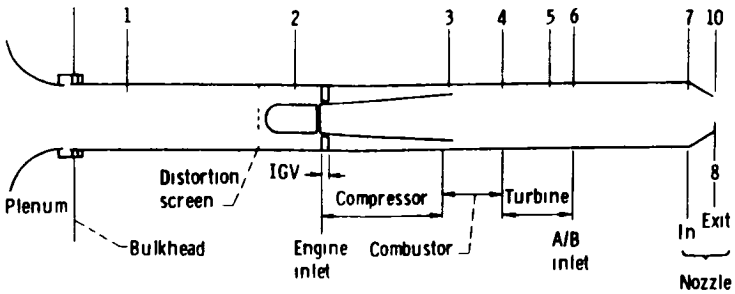

(a) Installation, flowpath schematic, and station designations

Figure 3 - Schematic of J85-21 engine, installation, and instrumentation

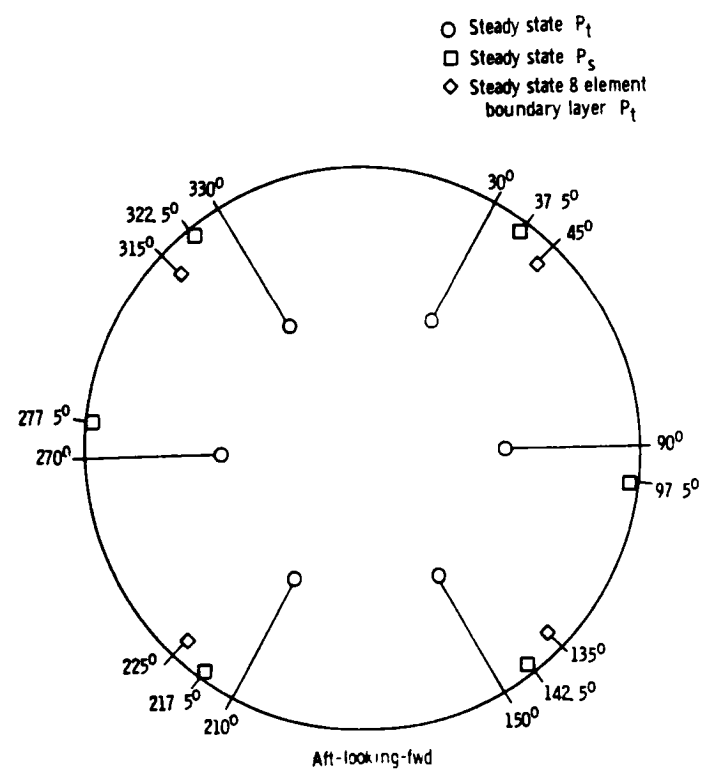

(b) Station 1

Figure 3 - Continued

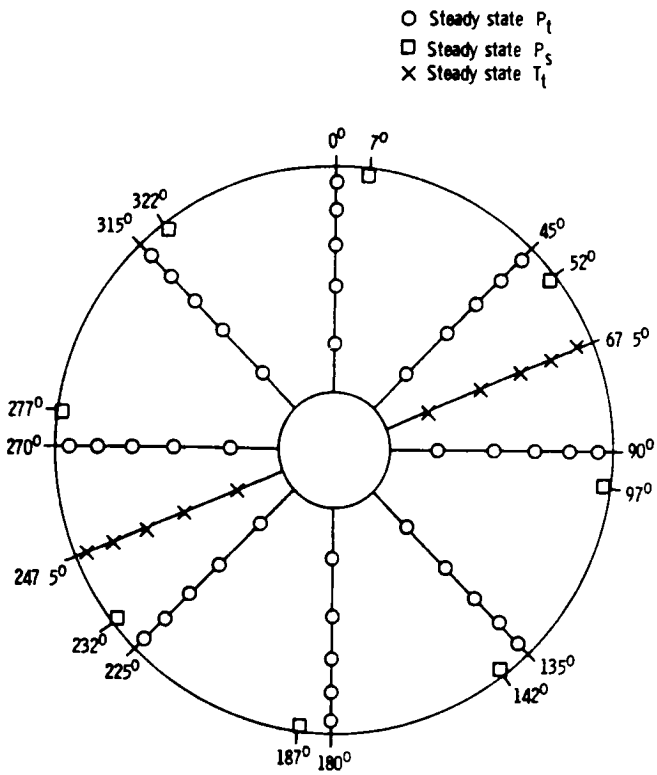

Aft-looking-fwd

(c) Station 2.

Figure 3 - Continued

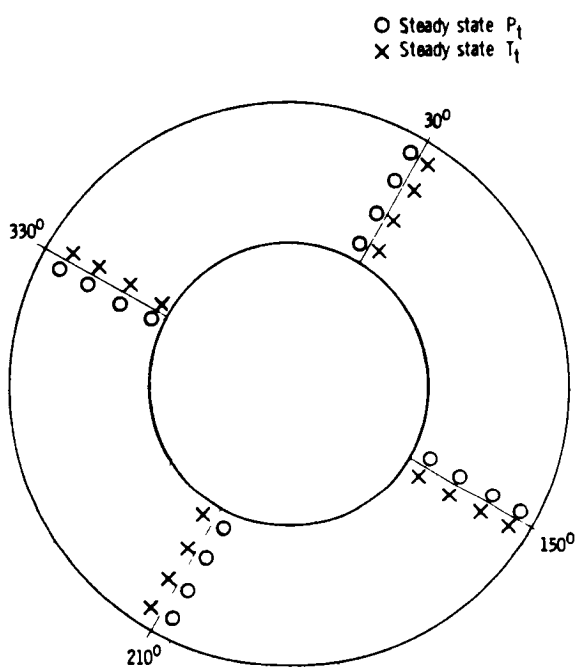

Aft-looking-fwd

(d) Station 3

Figure 3 - Continued

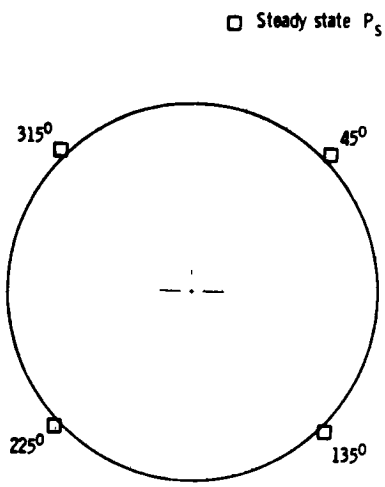

Aft-looking-fwd

(e) Station 10

Figure 3. - Concluded.

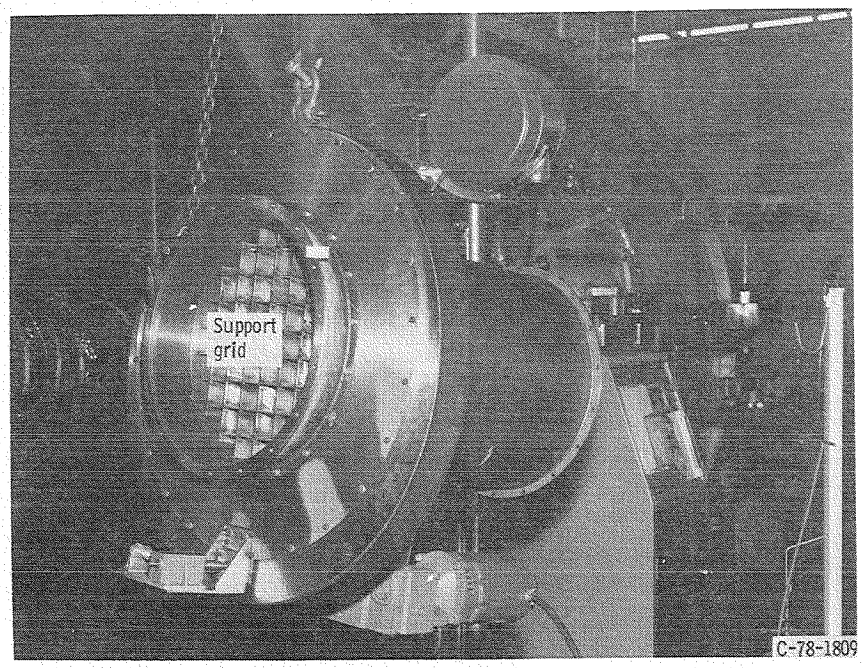

Figure 4. - Distortion screen support grid.

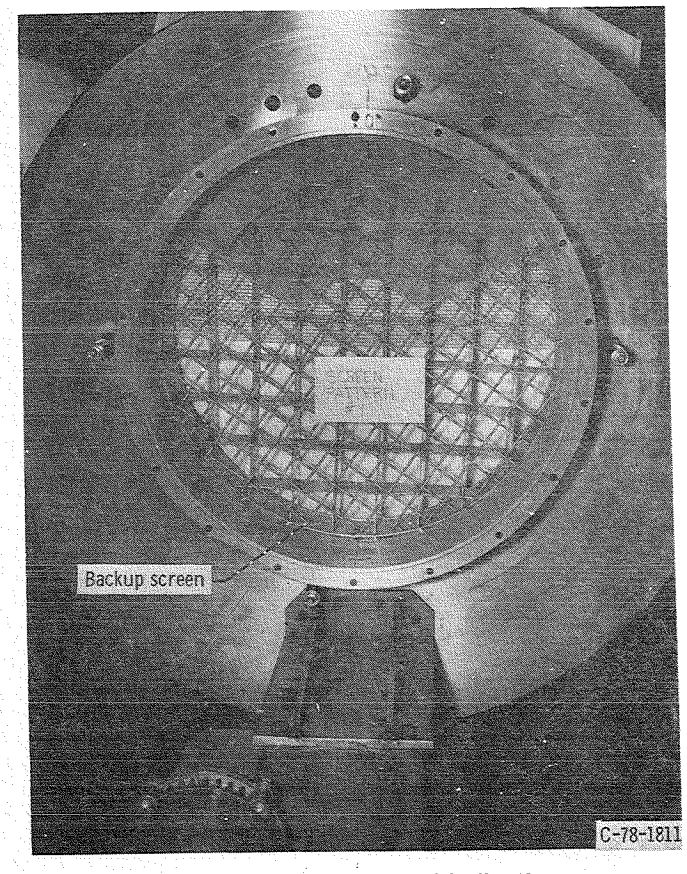

(a) Dense complex circumferential pattern 1.

Figure 5. - Distortion pattern photographs.

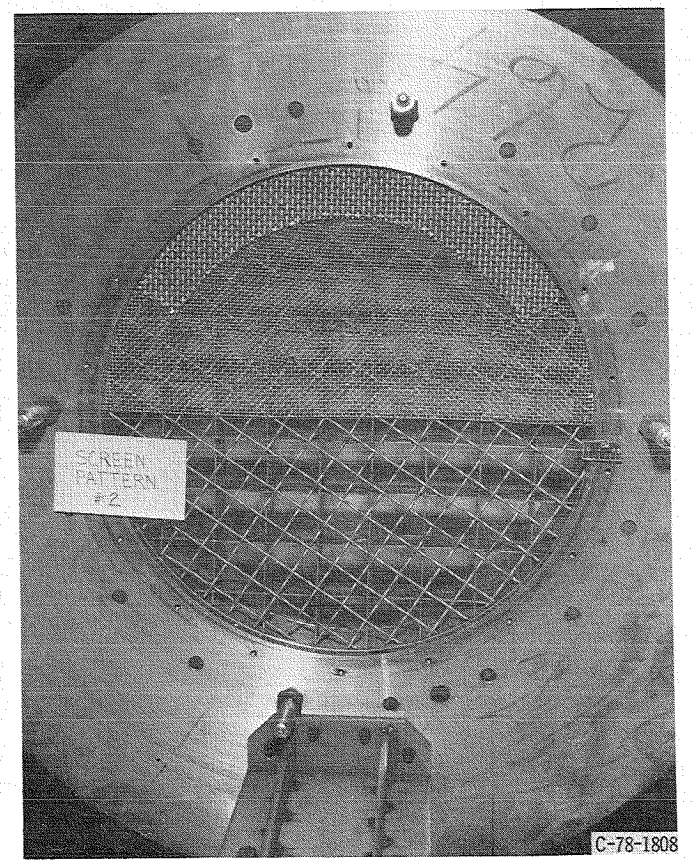

(b) Complex circumferential pattern 2.
Figure 5. - Continued.

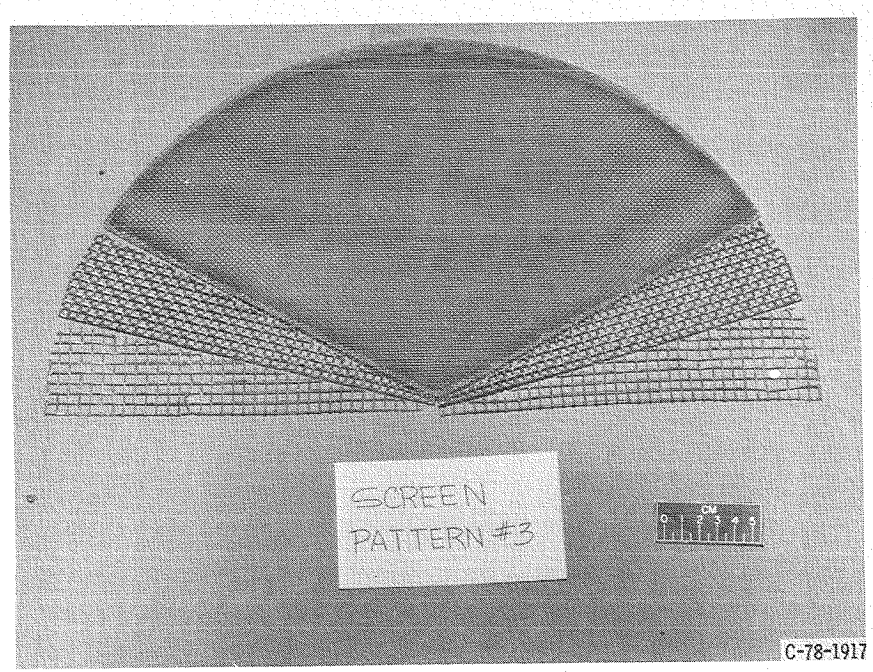

(c) 180° - Extent graded circumferential pattern 3.
Figure 5. - Continued.

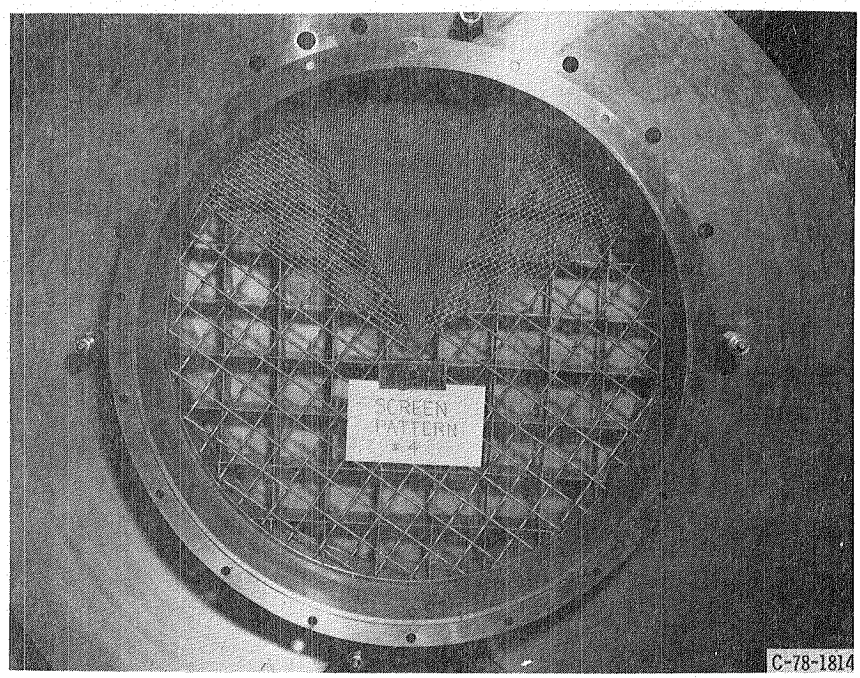

(d) 120° - Extent graded circumferential pattern 4.
Figure 5. - Continued.

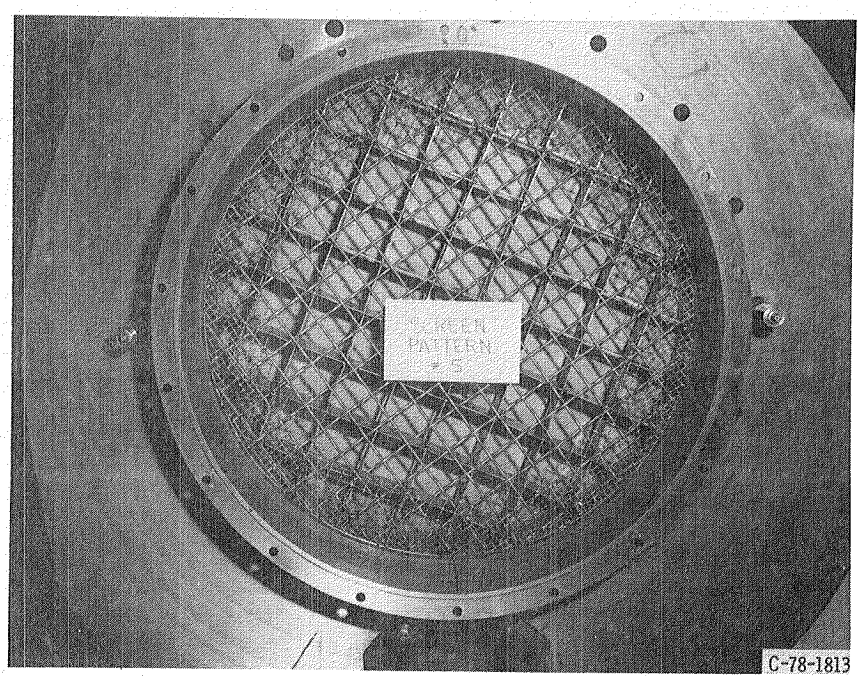

(e) Graded tip - radial pattern 5.
Figure 5. - Concluded.

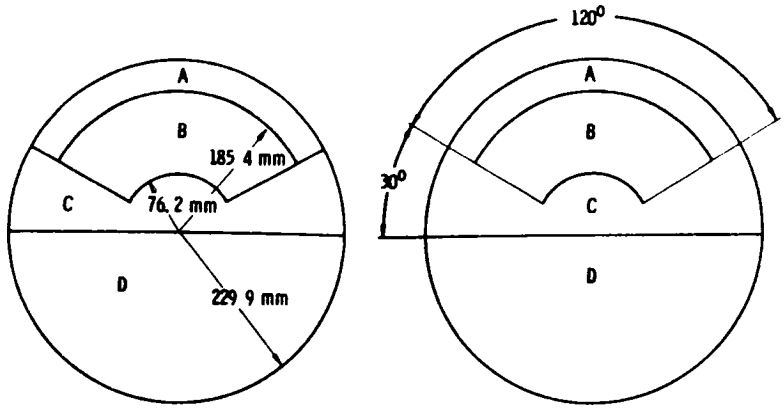

Pattern 1

Segment	Density
A	88.3%
B	65.8%
C	34.4%
D	0%

Pattern 2

Segment	Density
A	84.0%
B	44.6%
C	39.6%
D	0%

(a) Complex circumferential patterns

Figure 6. - Distortion pattern comparison

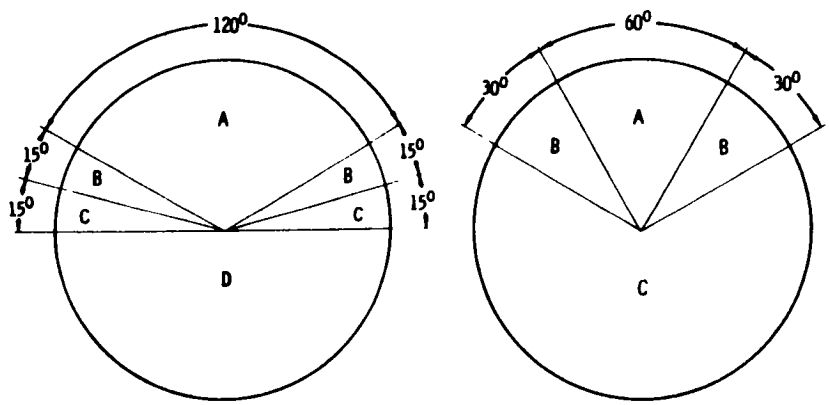

Pattern 3

Segment	Density
A	74.6%
B	52.1%
C	26.0%
D	0%

Pattern 4

Segment	Density
A	81.3%
B	53.1%
C	0%

(b) Graded circumferential patterns.

Figure 6. - Continued.

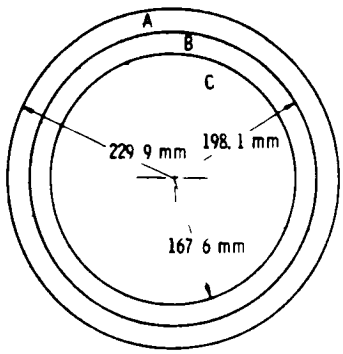

Pattern 5

Segment	Density
A	26 0%
B	17 9%
C	0%

(c) Graded tip-radial pattern

Figure 6. - Concluded

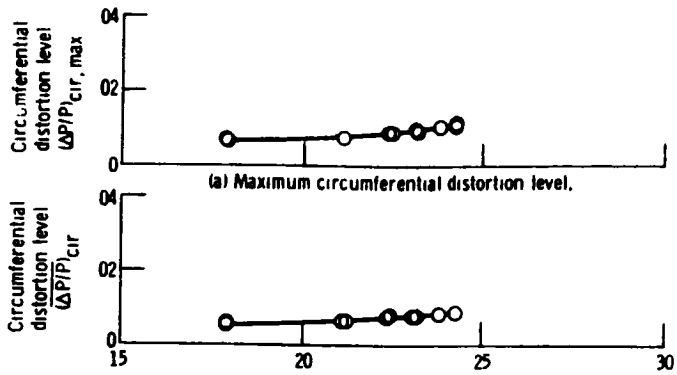

(b) Face-average circumferential distortion level

Figure 7 - Distortion level for clean inlet configuration

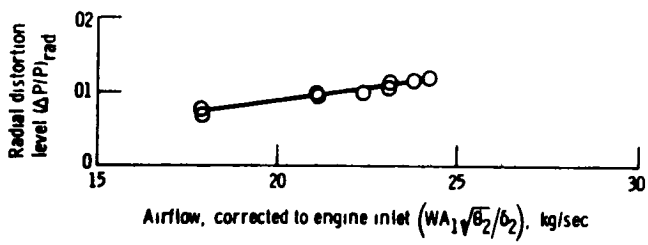

(c) Radial distortion level

Figure 7 - Concluded

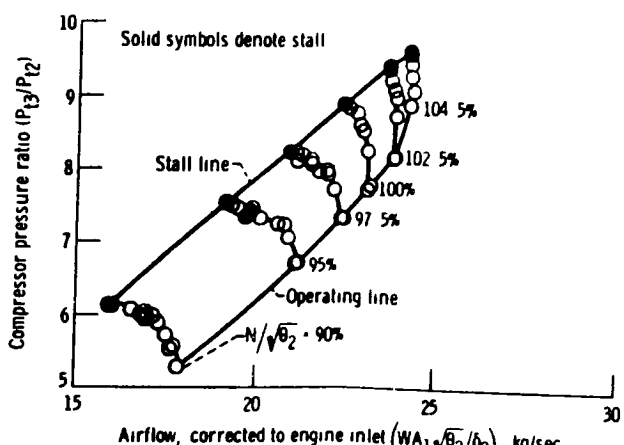

Figure 8 - Compressor performance with a clean inlet configuration

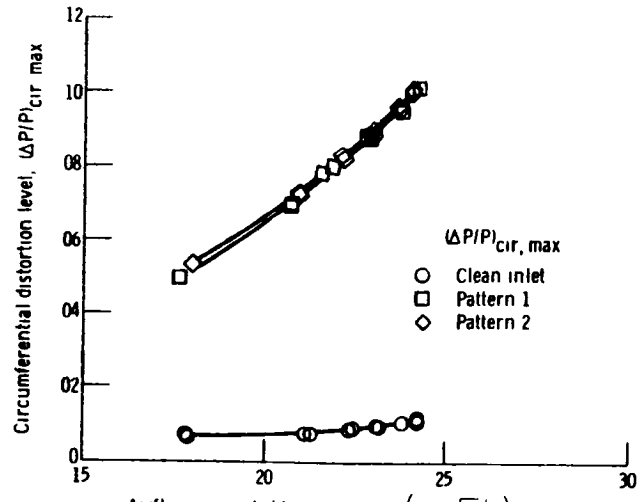

(a) Maximum circumferential distortion level

Figure 9 - Distortion level for complex circumferential screen patterns

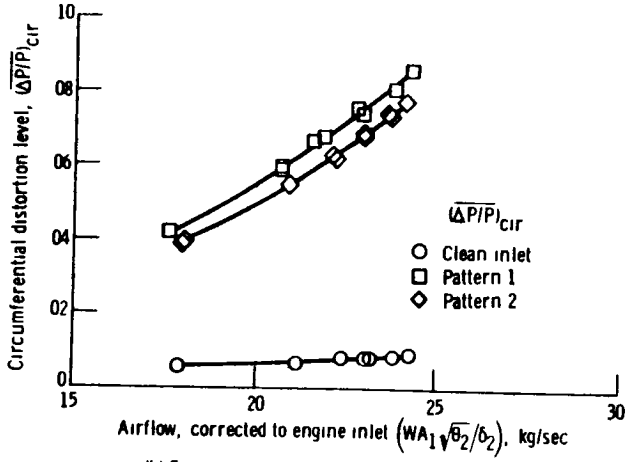

(b) Face-average circumferential distortion level

Figure 9 - Continued

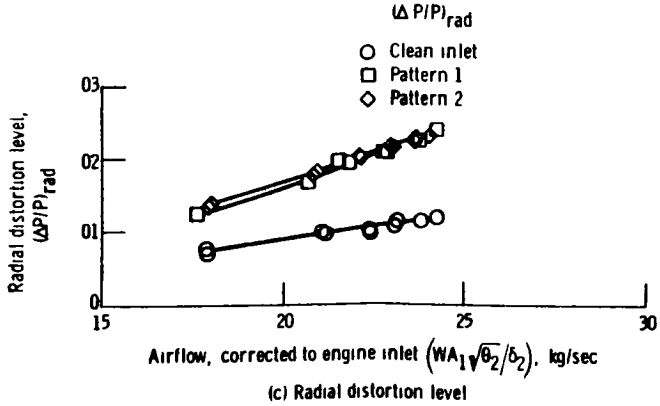

(c) Radial distortion level

Figure 9 - Concluded

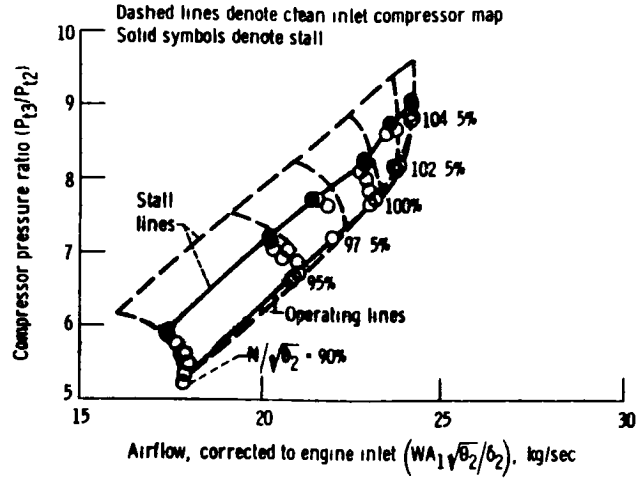

(a) Dense complex circumferential pattern 1

Figure 10 - Compressor performance with complex circumferential patterns

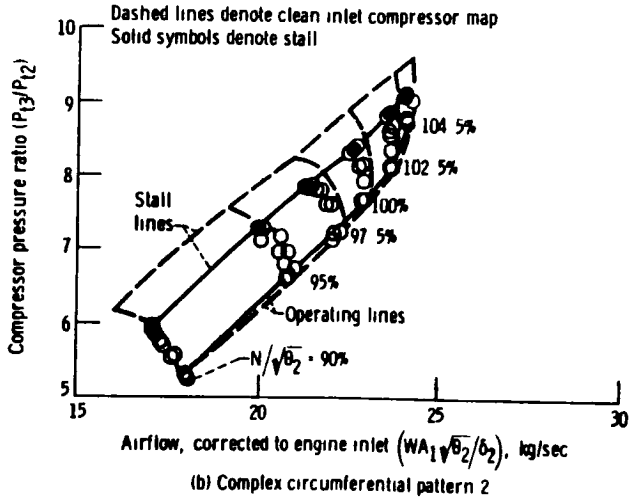

(b) Complex circumferential pattern 2

Figure 10 - Concluded

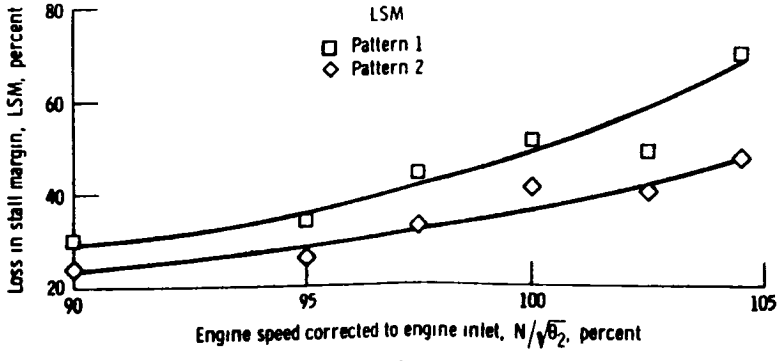

Figure 11 - Loss in stall margin for complex, circumferential patterns

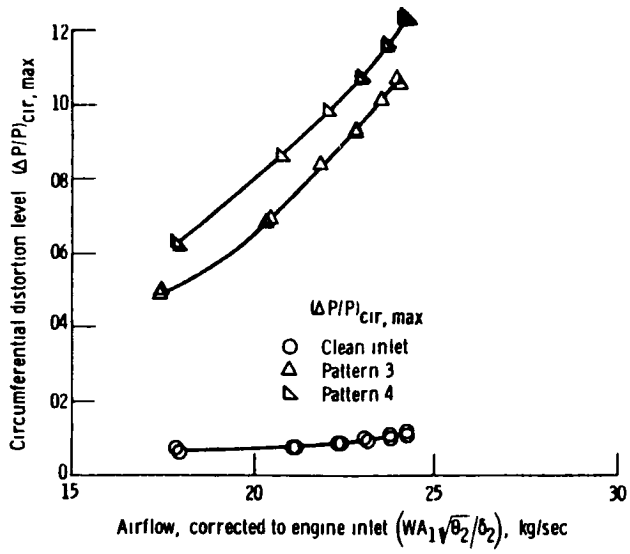

(a) Maximum circumferential distortion level

Figure 12 - Distortion level for graded circumferential screen patterns

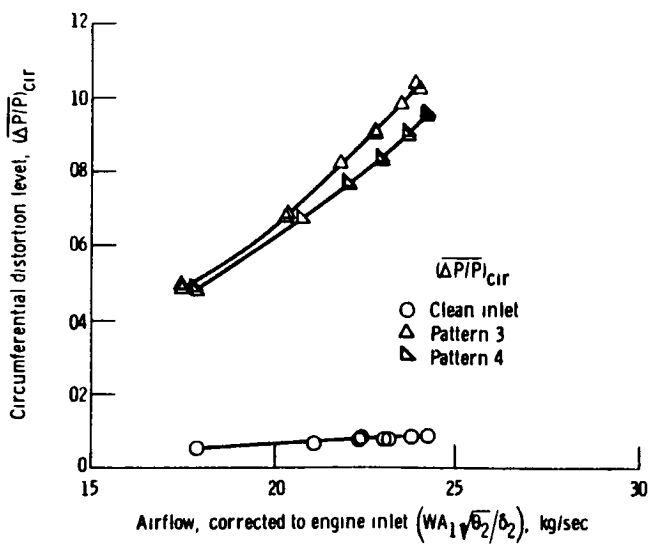

(b) Face-average circumferential distortion level

Figure 12 - Continued

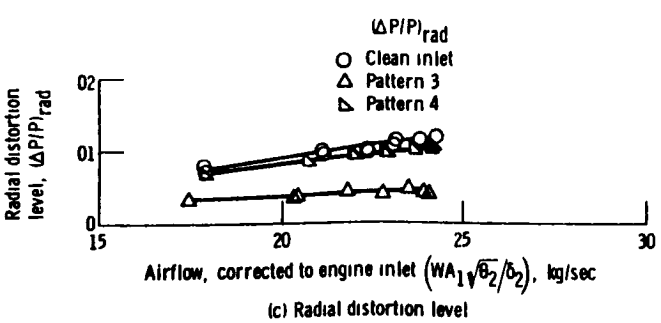

(c) Radial distortion level

Figure 12 - Concluded

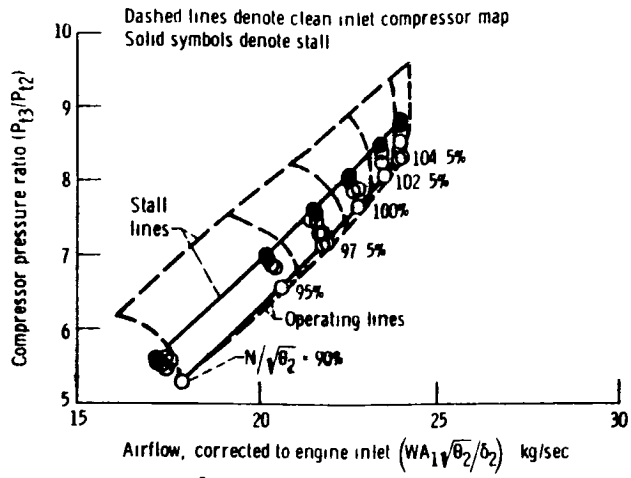

(a) 180°-Extent graded circumferential pattern 3

Figure 13 - Compressor performance with graded circumferential patterns

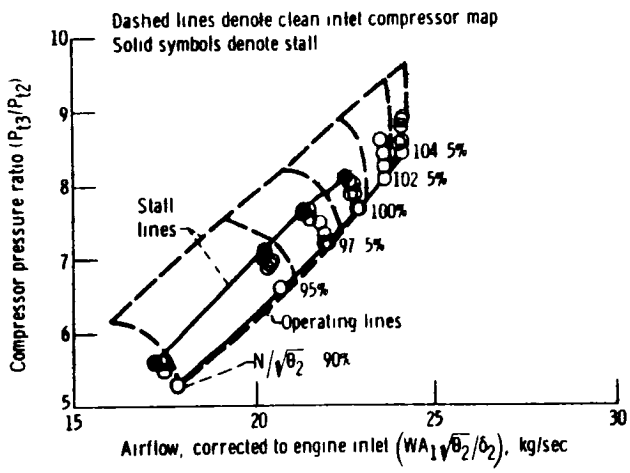

(b) 120°-Extent graded circumferential pattern 4

Figure 13 Concluded

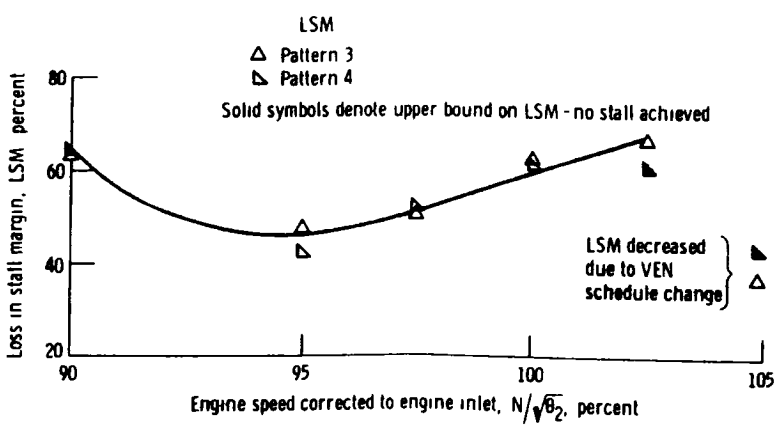

Figure 14 - Loss in stall margin for graded circumferential patterns

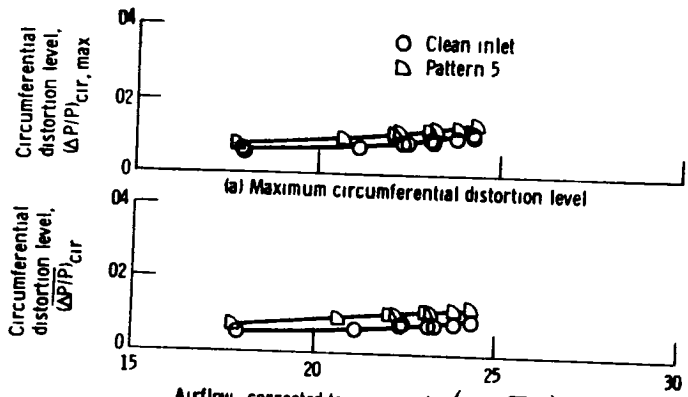

(a) Maximum circumferential distortion level

(b) Face-average circumferential distortion level.

Figure 15 - Distortion level for the graded tip-radial screen pattern

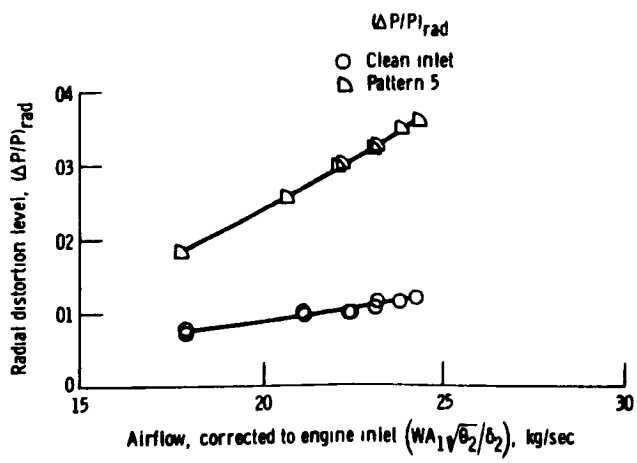

(c) Radial distortion level

Figure 15 - Concluded.

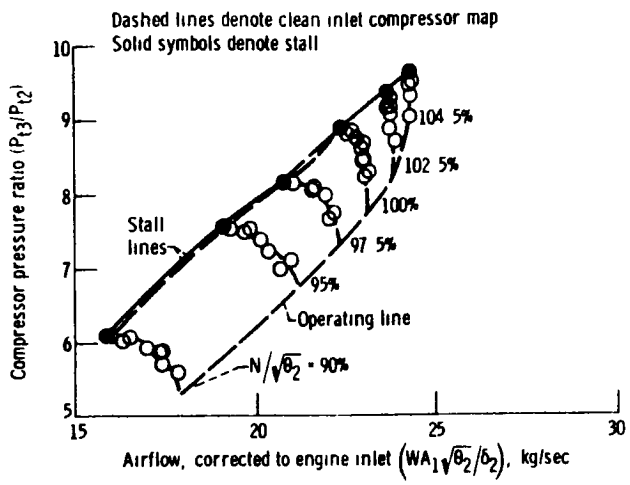

Figure 16 - Compressor performance with graded tip-radial pattern 5

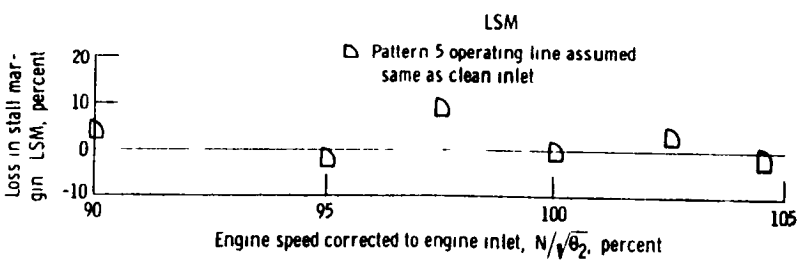

Figure 17 - Loss in stall margin for graded tip-radial pattern 5

End of Document